

5 **REVIEW**

10 **N-heterocyclic silylene complexes in catalysis:
new frontiers in an emerging field**

10 **Q1** Cite this: DOI: 10.1039/c3qi00079f

10 **Q2** Burgert Blom, Daniel Gallego and Matthias Driess*

15 The present account is a review of all N-heterocyclic silylene (NHSi) transition metal complexes that have been employed in catalytic transformations, reported up to the present time (2013). NHSi transition metal complexes now enjoy indefatigable attention since their facile isolation was realised by the report of the first isolable NHSis by West and Denk in 1994. Despite considerable research activity since then, in comparison to ubiquitous N-heterocyclic carbene (NHC) complexes, NHSi complexes are still comparatively rare. Accordingly, in comparison to the plethora of reports associated with NHC complexes, implicated in catalytic processes, only scant examples exist for NHSi complexes. Some of these reports include Heck or Suzuki type coupling, alkyne cyclotrimerisation, ketone hydrosilylation, amide reduction or Sonogashira cross-coupling reactions, and are discussed in detail here. These endeavours pave the way for new families of catalysts based on NHSis and highlight the potential future applications of these emerging and rather unexplored complexes in novel catalytic processes.

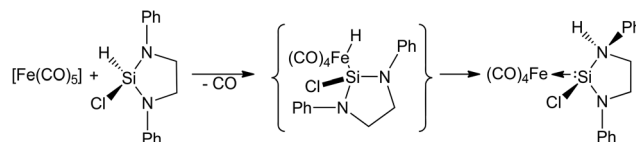
20 Received 23rd October 2013,
Accepted 5th December 2013

25 DOI: 10.1039/c3qi00079f

rsc.li/frontiers-inorganic

30 **Introduction**

Since the seminal work on the first N-heterocyclic silylene (NHSi) complex in 1977 by Welz and Schmid,¹ which was a thermolabile iron complex (Scheme 1), many subsequent NHSi complexes across the transition metals now exist. Despite these impressive efforts, in comparison, the number of reported N-heterocyclic carbene (NHC) stabilised complexes



30 **Scheme 1** Seminal example of an NHSi transition metal complex in 1977.

40 *Department of Chemistry, Metalorganics and Inorganic Materials, Technische Universität Berlin, Strasse des 17. Juni 135, Sekr. C2, D-10623 Berlin, Germany. E-mail: matthias.driess@tu-berlin.de*

40 still far out-weighs those based on NHSi ligands. This fact is most likely precipitated by the prevalence of the latter in key catalytic processes and their use in stabilising metal complexes in unusual oxidation states.²



45 **Burgert Blom**

with heavy main group element atoms and their reactivity.

45 *Burgert Blom obtained a Ph.D. degree from the University of Bonn (Germany) in 2011 in the field of metal-main group multiple bonding. He was awarded the Dr Edmund ter-Meer dissertation prize in 2012 and is currently a post-doctoral fellow in the group of Prof. Driess in Berlin. He is a member of the Universitätsgesellschaft Bonn and his main research area is exploring transition metal complexes forming reactive bonds*



45 **Daniel Gallego**

ligands as new scaffolds in supporting metals for catalysis.

45 *Daniel Gallego obtained a bachelor's degree with honours in Colombia from Universidad Nacional de Colombia. He then joined the joint Erasmus Mundus Master program ASC (Advanced Spectroscopy in Chemistry) in Lille (France) and Leipzig (Germany) where he obtained his Master's degree in 2011. Currently, he is a doctoral student in the group of Prof. Driess, exploring the use of novel bidentate NHSi and NHGe*

We have recently reported a comprehensive review of all existing N-heterocyclic silylene (NHSi) complexes of group IV through XII transition metal elements.³ We showed that these complexes represent an exciting new frontier which lies at the interface of ‘classical’ organometallic and contemporary main group chemistry, but can still be considered an emerging field. These emerging complexes have the ability to activate a range of small molecules in unique ways, highlighting their importance. Moreover, they possess the propensity to perform other interesting stoichiometric transformations, such as alkyne hydrosilylation mediated by a nickel based NHSi ligand, or silane activation, facilitated by a Ru NHSi complex, in addition to various other transformations.

In the present report, we wish to present a focussed and detailed discussion on NHSi complexes so far implicated *exclusively* in catalytic transformations, reported up to the present time (2013), and we will do so from a chronological perspective. Our group has been intensively involved in NHSi research in the last decade, and indeed most (but not all) of the examples of catalytically active NHSi complexes discussed here have evolved from these efforts. Only very few such examples exist to date, but these nevertheless show a “proof of concept” that NHSi ligands indeed hold promise as a new class of ligands likely to play an increasingly important role in future catalytic developments, and are certainly more than simple isoelectronic replacements for more traditional ligands.

Development of NHSi complexes as catalysts

Preliminary considerations

Transition metal silylene complexes can be classified into four distinct classes (Chart 1). Type **A** are analogues of Fischer or Schrock type carbene/alkylidene complexes ($L_nM = CR_2$), for example $[(CO)_4Os=Si\{S^pTol\}\{Ru(\eta^5-C_5Me_5)\}]$ or $[PtH(PCy_3)_2=Si(SET)_2]^+BPh_4^-$ reported by Tilley and co-workers in the 1990s.⁴



Matthias Driess

Matthias Driess obtained his Ph.D. degree in 1988 and completed his habilitation at the University of Heidelberg (Germany) in 1993. Since 2004 he is full professor at the Department of Chemistry of the Technische Universität Berlin (Germany). Since 2007 he serves as spokesperson of the Cluster of Excellence UniCat in the Berlin area. He received several awards, including the Wacker Silicone Award in 2010, and is a member of the

German National Academy of Sciences (Leopoldina). He has published more than 240 papers.

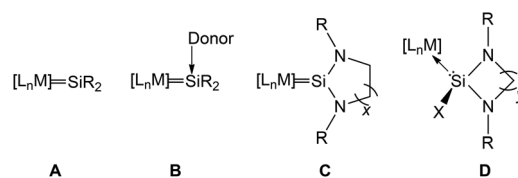


Chart 1 Transition metal silylene complexes categorised in four classes: in type **C** $x = 1$ or 2 ; $R =$ bulky aromatic or aliphatic group; in type **D** $y = 1, 2$ or 3 ; $X =$ a halogen or H ; $R =$ bulky aromatic or aliphatic group (adapted from ref. 3).

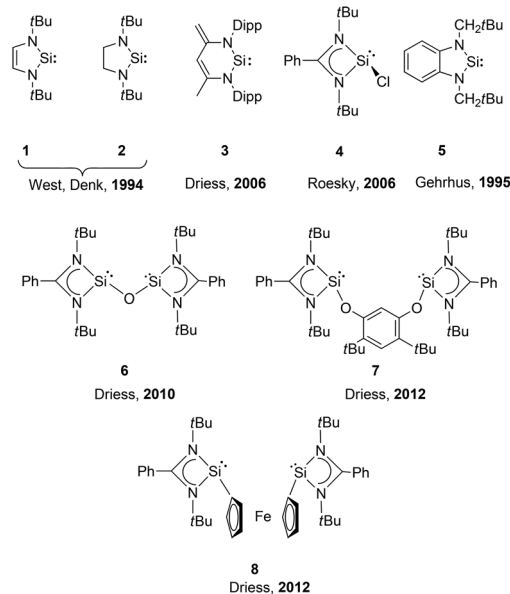


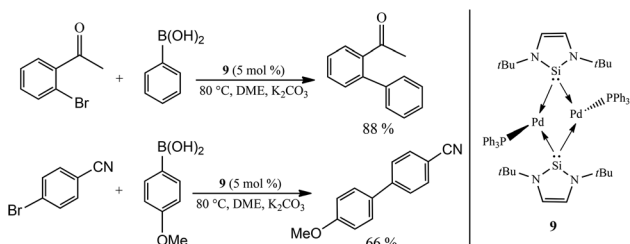
Chart 2 “Free” NHSi metallylenes as a new class of supporting ligands for new catalysts.

Type **B** represents “base stabilised” silylene ligands coordinated to transition metal fragments, exemplified by the seminal work of Zybill and co-workers: $[(CO)_4Fe=\{Si(OtBu)_2\leftarrow Donor\}]$ ($Donor = THF$ or $HMPA$).⁵ Members of type **C** represent NHSi complexes where unsaturated functionalities and/or additional R groups may exist in the ligand backbone, while type **D** represents NHSi halide or hydride complexes (Chart 2). We concentrate our discussion in this review on complexes belonging to classes **C** and **D** exclusively that have been shown to effect catalytic transformations.

Chart 2 provides an overview of the existing NHSi metallylene ligands, some of which have been employed in the synthesis of catalytically active metal complexes, and are used throughout the discussion in this review.⁶

A chronological account of catalytically active NHSi complexes

The first appearance of an NHSi complex implicated in a catalytic process was that by Fürstner and co-workers in 2001. They reported a novel dinuclear NHSi Pd complex prepared by treatment of **1** with $Pd(PPh_3)_4$ affording the complex $[Pd_2(\mu^2-1)_2(PPh_3)_2]$ (**9**).⁷ In this seminal work, two NHSi (**1**) ligands act as bridging ligands between the palladium centres forming a



Scheme 2 Seminal example of an NHSi complex (**9**) effectively enabling Suzuki cross-coupling reactions.

diamond-like core. Moreover, the dinuclear complex **9** was found to be effective in the Suzuki cross-coupling reaction of aryl boronic acids with bromoarenes (Scheme 2).

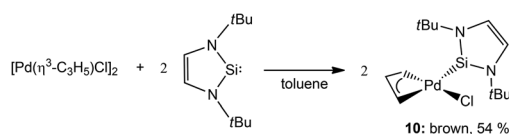
For the first time the ability of an NHSi to act as supporting ligands in a catalytically active complex was, perhaps fortuitously, uncovered.

It would take several more years for the next report to appear in this new area established by Fürstner and co-workers. In fact, only some seven years later did Roesky and co-workers communicate the second example of a catalytically active NHSi complex. They reported a mononuclear Pd-based NHSi complex obtained by reacting the NHSi **1** with the Pd precursor $[\text{Pd}(\eta^3\text{-C}_3\text{H}_5)\text{Cl}]_2$ affording $[\text{PdCl}(\eta^3\text{-C}_3\text{H}_5)(\leftarrow\text{1})]$ (**10**) in moderate yields (54%) (Scheme 3). Complex **10** was also found to be effective in the Heck coupling of styrene and bromoacetophenone.⁸ They also report a systematic study showing the effect of temperature on the yield of the coupled product, where at 140 °C, a 99% yield is achieved in 24 h, compared to 45% achieved in the same time at 80 °C.

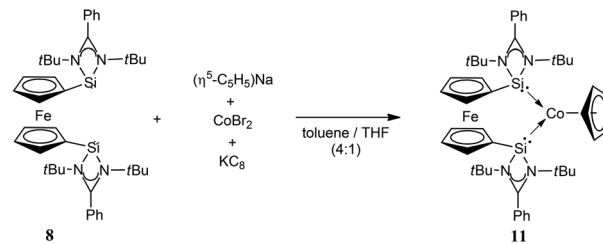
The effect of electron withdrawing/donating substituents on the catalyst rates was also systematically investigated by performing Heck coupling of various aromatic compounds with styrene. It was found that electron donating substituents on the aromatic ring generally afford lower yields of the coupled product, while electron withdrawing substituents result in higher yields.

Besides these two important examples, the remainder of the reports in this area stems from our group, given our prolonged interest in NHSis, and these reports have appeared recently and somewhat simultaneously.

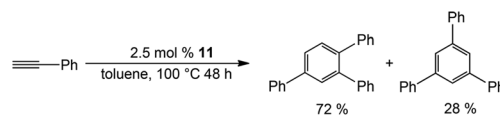
Accordingly, we first reported NHSi cobalt complexes, useful in catalysis, using our bidentate NHSi ligand, **8**, as a supporting chelating or even mono-dentate ligand.^{6g} The synthesis is straightforward and involves the reaction of $\text{Na}[\text{C}_5\text{H}_5]$ with anhydrous CoBr_2 , in the presence of a reducing agent (KC_8), along with **8** (Scheme 4). This procedure affords the



Scheme 3 Synthesis of the second example of an NHSi complex (**10**) as an active Heck coupling pre-catalyst.



Scheme 4 Synthesis of the novel cobalt-based bis-NHSi complex **11**. The Ge analogue (**12**) can also be accessed in an analogous way.



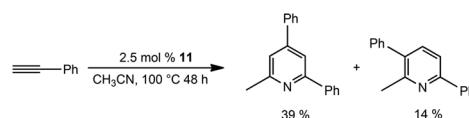
Scheme 5 Catalytic cyclotrimerisation using bis-silylene Co complex **11** as a pre-catalyst.

complex $[(\eta^5\text{-C}_5\text{H}_5)\text{Co}(\eta^2\text{-8})]$ (**11**), which features a resonance signal in the ^{29}Si NMR spectrum at $\delta = 82.0$ ppm, and is down-field shifted from that of the free ligand ($\delta = 43.3$ ppm) **8**, as expected for coordination. In close analogy, the Ge analogue of **11** can also be accessed synthetically (**12**).

Complex **11** is catalytically active in the $[2 + 2 + 2]$ cyclotrimerisation reaction of phenylacetylene, yielding two isomeric forms of triphenylbenzene (Scheme 5), while surprisingly **12** is inactive catalytically. A plausible reason was proposed for the inactivity of the latter: stronger coordination of the Ge atoms to Co, thereby hampering alkyne coordination to the Co centre, an obvious key step in the catalytic process. This seemed reasonable given the lack of detailed mechanistic studies on this system in this report. However, it was shown in a subsequent study (*vide infra*) that Si is more strongly coordinating, so most likely the catalytic inactivity of **12** is a consequence of instability under the catalytic conditions, rather than an effect of coordination strength.

Remarkably, repeating the cyclotrimerisation catalysis of phenylacetylene in CH_3CN as a solvent, mediated by **11** as a catalyst, affords substituted pyridines in moderate yields (Scheme 6).

The reaction of silylene **8** with two molar equivalents of $[(\eta^5\text{-C}_5\text{H}_5)\text{Co}(\text{CO})_2]$ in hexane accordingly affords the related dinuclear Co complex **13**, with concomitant loss of two equivalents of CO (Fig. 1). However, in the case of complex **13**, no catalytic studies were undertaken, but it principally also represents a potentially active catalyst precursor, and could facilitate mechanistic investigations into this catalyst process.



Scheme 6 Catalytic formation of pyridines using bis-silylene Co complex **11** as a pre-catalyst in CH_3CN .

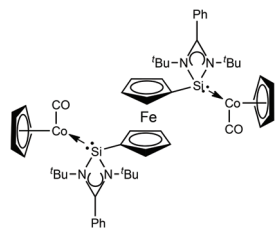


Fig. 1 Structure of dinuclear Co complex **13** based on NHSi **8**.

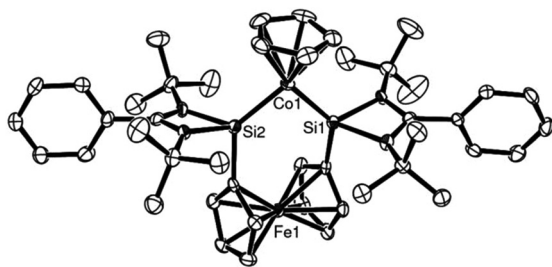
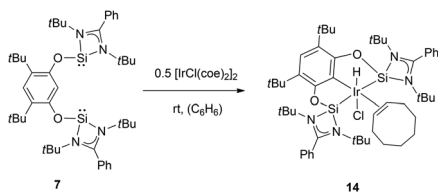


Fig. 2 ORTEP representation of complex **11**: an active alkyne cyclo-trimerisation catalyst precursor. (Thermal ellipsoids at 50% probability, H atoms omitted for clarity.)

The X-ray structure of complex **11** was in accord with the spectroscopic findings and is shown in Fig. 2. The rather short Co–Si bond lengths (2.1252(14) and 2.1200(14) Å respectively) hint at a rather strong σ -donor ability of ligand **8**.

On continued exploration of the versatility of the NHSi **4**, the first pincer bis-NHSi was obtained in our group by its salt metathesis reaction. We explored the coordination ability of **7** to an iridium centre, obtaining the octahedral complex [SiCSi]–IrHCl(coe) (**14**) by oxidative addition of an aromatic C–H bond in **7** with 0.5 molar equivalent of [IrCl(coe)₂]₂ (Scheme 7). In this work, we found that complex **14** served as a pre-catalyst for the C–H borylation of arenes using pinacolborane (HBPin).⁹ For comparative purposes, we also prepared a series of iridium pincer complexes with the Ge analogue (**15**) and two phosphane-based ligands: *t*Bu₂P and the more electronically related (iPrNCH₂)₂P (**17** and **18** respectively, Scheme 8). The catalytic evaluation of this series showed an interesting contrast between the metallylenes *versus* the phosphane based pincer ligand systems. We found that both **14** and **15** are substantially more effective in this catalytic transformation compared to the isoelectronic P(III) analogues **17** and **18** (Table 1), highlighting the fact that the use of Si or Ge as donor ligands



Scheme 7 Synthesis of the iridium NHSi complex **14**, a pre-catalyst active in the C–H borylation of arenes using HBPin.



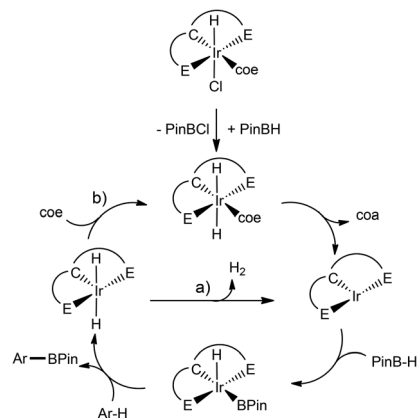
Scheme 8 Synthesis of the iridium P(III) analogues of complex **14**, for comparison in the catalytic C–H borylation of arenes.

Table 1 Catalytic yields (%) for the borylation of arenes using the pincer complexes **14**, **15**, **17** and **18** as precatalysts. Yields in bold are without the presence of COE

Arene	14	15	17	18
	ArBPIn: 90 coaBPIn: 3 coeBPIn: 1 ArBPIn: 53	ArBPIn: 80 coaBPIn: 9 coeBPIn: 8 ArBPIn: 46	ArBPIn: 64 coaBPIn: 11 coeBPIn: 7 ArBPIn: 60	ArBPIn: 21 coaBPIn: 35 coeBPIn: — ArBPIn: 55
	ArBPIn: 91 (m : p = 1.6 : 1) coaBPIn: 3 coeBPIn: 3 ArBPIn: 16	ArBPIn: 39 (m : p = 1.5 : 1) coaBPIn: 8 coeBPIn: 7 ArBPIn: 12	ArBPIn: 40 (m : p = 1.4 : 1) coaBPIn: 49 coeBPIn: 10 ArBPIn: 9	ArBPIn: 9 (m : p = 1.4 : 1) coaBPIn: 34 coeBPIn: — ArBPIn: 20
	ArBPIn: 15 coaBPIn: 19 coeBPIn: 26 ArBPIn: 11	ArBPIn: 4 coaBPIn & coeBPIn: <5 ArBPIn: 5	ArBPIn: 10 coaBPIn & coeBPIn: <5 ArBPIn: 8	ArBPIn: 11 coaBPIn: 25 coeBPIn: 23 ArBPIn: 23
	ArBPIn: 11 coaBPIn: 30 coeBPIn: 50 ArBPIn: 10	ArBPIn: 6 coaBPIn & coeBPIn: <5 ArBPIn: 3	ArBPIn: 17 coaBPIn & coeBPIn: <5 ArBPIn: 4	ArBPIn: 5 coaBPIn: 20 coeBPIn: — ArBPIn: 19
	ArBPIn: 0 —	ArBPIn: 0 —	— —	— —

plays a substantial role in the catalytic activity, and are not simple isoelectronic substitutes. The latter (Si and Ge) are much stronger σ -donor ligands, which tune the catalytic activity in this key catalytic process.

A positive effect on the turnover frequency (TOF) and number (TON) was obtained while an additional equivalent of the co-ligand/hydrogen acceptor COE was added to the catalytic system using **14** and **15** as pre-catalysts. For instance, when benzene was used as the substrate the TON increased *ca.* twice its value (TON: 9–10 without COE and 16–18 with COE). On the other hand, this effect was higher on the TOF after 3 h of reaction, since almost all of the substrate was consumed in the presence of COE (TOF_{3h}: 1.3 h⁻¹ without COE and 5.3 h⁻¹ with COE). This result suggested that COE plays a crucial role in kinetic stabilization of the active species. In contrast, addition of COE to the C–H borylation reactions using **17** or **18** as



Scheme 9 Proposed mechanism for the C–H borylation of arenes by [ECE] Ir-pincer complexes (E = Si, Ge, P).

pre-catalysts either had little (**17**) or a detrimental effect on the overall catalytic performance, affecting the selectivity of the reaction towards borylation of the olefin (**18**) (Table 1).

A general landscape for the mechanism is depicted in Scheme 9. The activation of the pre-catalyst occurs in the presence of HBPn to produce the dihydride species which undergoes concomitant hydrogenation of COE to produce the Ir(I) active species. An oxidative addition of HBPn to Ir(I) occurs subsequently to activate the aromatic C–H bond, forming ArBPn and {Ir(III)(H)₂} either by oxidative addition/reductive elimination or a σ -bond metathesis reaction. Finally, the Ir(I) active species can be obtained either by (a) release of H₂ or (b) COE coordination to the free site of this species and its further hydrogenation. A competitive reaction is present where a borylation of the olefin occurs instead. The difference in activity of **14** and **15** comes from the fact that in using bis-NHSi or bis-NHGe, the Ir centre is more electron-rich than with the phosphine ligands, increasing the activation barrier for the reductive elimination to produce H₂. Thus, addition of COE produces a beneficial effect on the catalytic performance.

In addition to the difference in reactivity of pincer metallacyclic ligands versus the well known phosphine ligands, X-ray structural (Fig. 3) and NMR spectroscopic analyses for complexes **14**, **15**, **17** and **18** revealed the markedly stronger σ -donor properties of bis-NHSi (Table 2). According to the Chatt–Dewar–Ducanson bonding model, when the electronic density on a metal center increases, the π -backbonding to the C=C bond is more pronounced. This drives to an elongation on the olefinic bond as well as a high-field chemical shift in the NMR spectra for both, the protons and ¹³C nuclei involved. Therefore, the order of σ -donor strength on this series of pincer ligands could be drawn as follows: SiCSi > GeCGe > iPrN-PCP > *t*Bu-PCP.

Based on the interesting properties presented by the complexes **14** and **15** with iridium as the metal centre, we expanded the scope to group 10, specifically nickel as a non-precious transition metal centre. The nickel pincer complexes with **7** as ligand the bis-germylene analogue and isoelectronic bis-phosphane ligands (**19**, **20** and **21** respectively) were

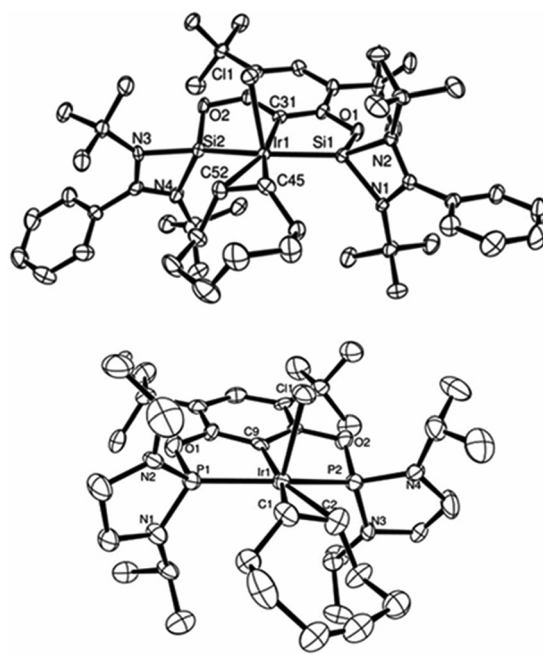
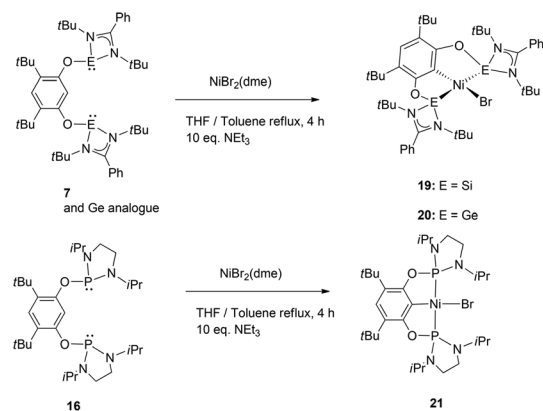


Fig. 3 ORTEP representation of complexes **14** (top) and **18** (bottom): pre-catalysts for the C–H borylation of arenes using HBPn. (Thermal ellipsoids at 50% probability, H atoms omitted for clarity.)

Table 2 Analytic data for the olefinic bond C=C on the [ECE]IrHCl(coe) complexes (E = Si, Ge, P)

Analytic method	14	15	18
X-ray diffraction (XRD) $d(\text{C}=\text{C})$ (Å)	1.409(9)	—	1.35(1)
¹ H NMR C=C–H	3.38	4.06	4.31
¹³ C NMR C=C	55.8	65.1	81.6



Scheme 10 Synthesis of complexes **19–21**.

obtained by a C–H activation with NiBr₂(dme) as a precursor (Scheme 10 and Fig. 4) in high yields under an excess of a base.¹⁰

Interestingly, we observed that these complexes can act as a catalyst for the Sonogashira cross-coupling reaction between phenylacetylene and 1-octenyl iodide in moderate yields

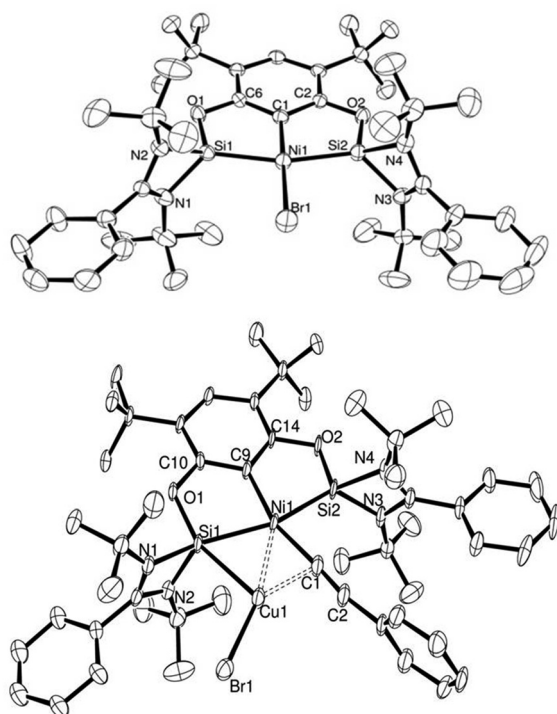
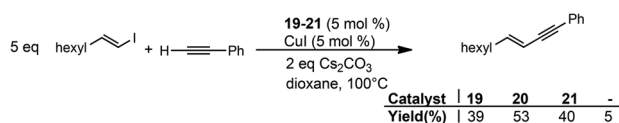


Fig. 4 ORTEP representation of complex **19** (top) and **22** (bottom). Thermal ellipsoids set at 50% probability level, H atoms omitted for clarity.



Scheme 11 Catalytic evaluation of complexes **19–21** in the Sonogashira cross-coupling reaction.

(Scheme 11). Direct comparison with a blank test, without any catalyst but with added CuI showed that indeed the nickel complexes are the active coupling catalyst. In this case just stoichiometric formation of the coupling product was induced by the Cu(I) salt.

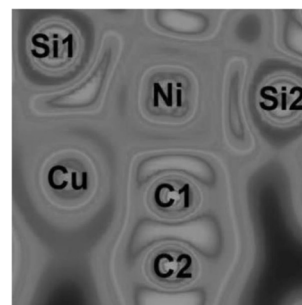
Variations on the catalytic conditions were tested without any improvement neither on the TON nor on the TOF. These pre-catalysts represent additional examples of the rather rare nickel-catalysed Sonogashira cross-coupling reaction,¹¹ making them somewhat remarkable. Moreover, the catalytic activity is in the same range of the phosphine-based catalyst, suggesting that most probably the medium activity does not depend on the sensitivity of the catalytic system. We next sought to understand in more detail whether these complexes were stable under the different chemical transformations potentially occurring in the catalytic cycle, and thereby shed light on the mechanism.

We evaluated our system through the sequence of transmetalation→oxidative addition→reductive elimination in stoichiometric amounts and analysed, when possible, the reaction

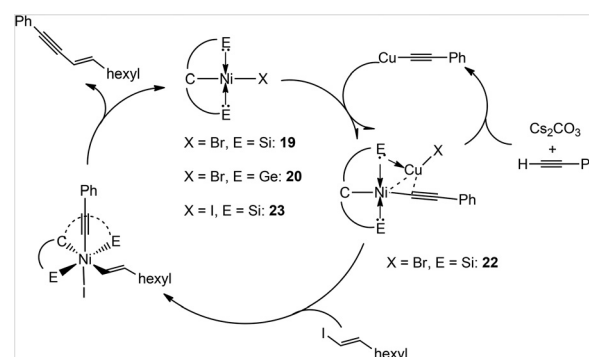
intermediates. Transmetalation with copper acetylides and the nickel complexes showed an equilibrium reaction between reagents and products. More importantly, we found that these ligands enabled the isolation and structural characterisation of the transmetalation product, in which the formed CuBr is bound to one of the NHSi arms and the acetylide ligand (**22**: {7:→Ni-CC-Ph→CuBr}) (Fig. 4).

We also evaluated this unusual structure through detailed DFT calculations focusing on the Electron Localization Function (ELF) and Mayer Bond Order (MBO). These results showed a two-electron three-centered system between Cu-Si-Ni (Scheme 12). In addition, the CuBr is coordinated in an end-on fashion to the acetylide coligand according to the MBO values.

For the further analysis of the next step (oxidative addition→reductive elimination), we reacted the *in situ* generated **22** with three molar equiv. of *E*-1-octenyl iodide at 50 °C for 2 h. By NMR analysis we found the formation of the coupling product in high yields (>90%) and a compound with similar features to the starting catalyst. Independent synthesis of the expected [SiCSi]NiI complex (**23**) (see Scheme 13) showed that the species formed are in accord with an oxidative addition→reductive elimination pathway. The reaction intermediate for this chemical transformation was elusive, although the retention of the stereochemistry on the C=C bond on the product suggested that this is the most likely pathway.



Scheme 12 ELF plot in the main Ni coordination plane for [7:→Ni-CC-Ph→CuBr] (**22**) (adapted from ref. 10).



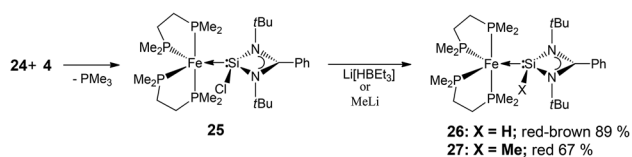
Scheme 13 Proposed catalytic pathway for in the Sonogashira cross-coupling mediated by **19** and **20** (pincer ligand is represented as E-C-E, E = Si, Ge).

Based on these stoichiometric studies a general reaction mechanism can be depicted as follows (Scheme 13): the [ECE]-NiBr complexes react with copper phenylacetylide producing the adducts $\{[ECE]Ni-CC-Ph \rightarrow CuBr\}$ (22). The latter reacts further with the (*E*)-1-octenyl iodide either by (a) oxidative addition–reductive elimination or (b) radical pathway. At the end the product (*E*)-dec-3-en-1-ynylbenzene is liberated and the cycle is closed.

Around the same time as the aforementioned reports from our group, we also focussed our attention on iron, particularly given its abundance, low cost and recent burgeoning interest in its use in other catalytic processes not based on NHSis.¹² To our surprise, only three iron-based NHSi complexes had been previously reported,¹³ all bearing the electron withdrawing $\{Fe(CO)_4\}$ moiety, and no catalytic transformation mediated by these complexes had been reported. This apparent gap in the literature encouraged us to explore a potentially *more* electron-rich iron fragment, other than $\{Fe(CO)_4\}$, to which an NHSi could potentially coordinate, and thereby, due to the increase in electron density at Fe, increasing the reactivity of the emerging complex.

In this regard, we found the precursor complex $[Fe(dmpe)_2(PMe_3)]$ (24),¹⁴ (dmpe = 1,2-bis(dimethylphosphino)ethane) a particularly attractive candidate since it has been shown to undergo facile PMe_3 loss upon reaction with a variety of other unsaturated low-valent main group compounds, affording multiply bonded Fe–E (E = Ge or Sn) adducts.¹⁵ Inspired in part by this, we carried out the reaction of 24 with NHSi 4 which indeed affords by PMe_3 loss the corresponding NHSi complex $[(dmpe)_2Fe \leftarrow :4]$ (25) (Scheme 14) as the first example of an electron-rich iron NHSi complex. Moreover, this complex can readily be converted by hydride–halogen exchange to the hydrido silylene complex 26 (Scheme 14), representing a very rare example of a Si(II) hydride coordinated to a metal centre.¹⁶

Complexes 25 and 26 both exhibit trigonal bipyramidal geometries in the solid state, according to single crystal XRD studies (Fig. 5 and 6). The NHSi ligands reside in one of the equatorial positions which is a preferred position for a π -acidic ligand in a trigonal bipyramidal coordination sphere, suggesting possible π -back-bonding from Fe to Si in both complexes (Table 3). Moreover, the Fe–Si bond lengths in both complexes are comparatively short, and in fact comparable to other reported iron silylene complexes of the type $L_nFe=SiR_2$ (2.154(1) Å, in complex $Cp^*COTMSFe=SiMes_2$;



Scheme 14 Synthesis of the NHSi iron complex 25, using a PMe_3 elimination strategy, and subsequent H, Cl or Me exchange with Superhydride[®] and CH_3Li affording the hydrido and methylated NHSi-complexes 26 and 27, respectively.

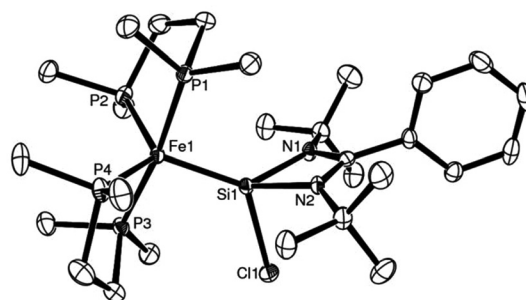


Fig. 5 ORTEP representation of complex 25: Thermal ellipsoids at 50% probability, H atoms omitted for clarity (adapted from ref. 16).

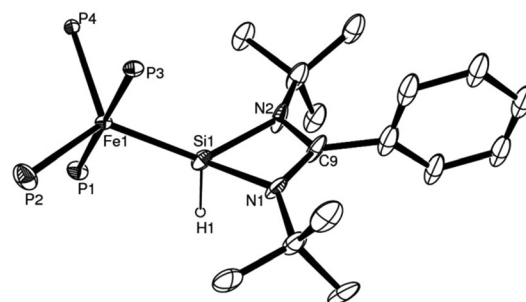


Fig. 6 ORTEP representation of one of the stereoisomers found in the asymmetric unit of complex 26: thermal ellipsoids at 50% probability, H (except H1) atoms and carbon atoms of the dmpe ligands omitted for clarity (adapted from ref. 16).

Table 3 Summary of some key metrical parameters in complex 25 and 26

	$d(Fe-Si)/\text{\AA}$	$d(Si-X)^a/\text{\AA}$	$d(Si-N1)/\text{\AA}$	$d(Si-N2)/\text{\AA}$
25	2.1634(9)	2.2281(11)	1.920(2)	1.931(2)
26	2.184(2)	1.50(2) ^b	1.930(6)	1.915(7)

Cp^* : 1,2,3,4,5-pentamethylcyclopentadienyl; TMS: $SiMe_3$; Mes: 2,4,6-trimethylphenyl).¹⁷

Complex 26 exhibits substantial statistical disorder in the X-ray structure solution, which was resolved as two independent stereoisomers in the asymmetric unit. This phenomenon is likely attributable to an increase in the energy barrier of the Berry pseudorotation (BSR), which affords two coexisting stereoisomers, under crystallisation conditions at low temperatures. This is not the case with its precursor, complex 25, highlighting a difference in the behaviour of the two complexes. The increase in the BSR barrier was additionally elucidated by $^{31}P\{^1H\}$ NMR spectra where at room temperature a relatively sharp singlet signal is observed for complex 25, suggesting fluxional exchange of the P_{axial} and $P_{equatorial}$ atoms on the NMR time scale. Complex 26, on the other hand at the same measuring frequency and temperature, exhibits a very broad signal in the $^{31}P\{^1H\}$ NMR spectrum, pointing to a substantial increase in the energy requirements for the P_{axial} and $P_{equatorial}$ exchange on NMR time scale.¹⁸ Moreover, progressive

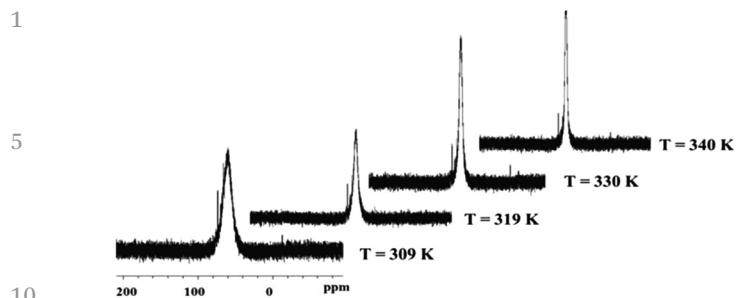


Fig. 7 Variable temperature $^{31}\text{P}\{^1\text{H}\}$ NMR spectra of **26**.

sharpening of this signal occurs on increasing the temperature as shown by variable temperature NMR investigations, which were also carried out (Fig. 7).

A further key spectroscopic feature of complex **26** is the existence of the silicon bound hydride atom. Due to the sluggish pseudorotation of the dmpe groups at room temperature, its chemical shift position could not obviously be located in the ^1H NMR spectrum, due to its being hidden by aromatic resonance signals, as a complex multiplet (a triplet of triplets). A two dimensional Si,H spectrum, however showed a weak cross peak confirming its presence (Fig. 8). Moreover, on heating the sample, and with onset of pseudorotation (see above), a quintet multiplicity for the Si-H is observed, as a result of $^3J(\text{Si},\text{P})$ coupling to four equivalent P atoms, further confirming its presence.

The ^{29}Si NMR shifts of complex **25** appear at $\delta = 43.1$ and that of complex **26** at $\delta = 63.6$ ppm. The related methylated complex **27**, also prepared in this study (Scheme 14), exhibits a resonance signal at $\delta = 102.5$ ppm. These values are related linearly to the respective Hammett-constants of the substituents at the Si centre,¹⁹ and can further be rationalised on the basis of Bent's rule.²⁰ In all cases the signals appear as quintets, as a result of $^2J(\text{Si},\text{P})$ coupling to P atoms, rendered equivalent, as a consequence of BSR.

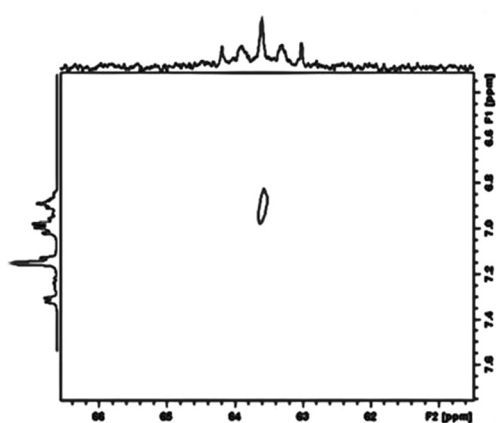


Fig. 8 Two dimensional H, Si correlation spectrum (COSY) of complex **26** showing a weak cross peak for the Si signal and the Si bound hydride atom, confirming its connectivity to Si.

Detailed DFT studies of complexes **25–27** were also reported (B3LYP/6-31G(d) for C, H, N, Cl and Si; LANL2DZ for Fe), to gain further insights into the bonding, in this study. Noteworthy is that in all cases the HOMO reflects π -back-bonding between the iron and silicon atoms, providing some explanation for the bond length contraction observed in the structural investigations. What is particularly of importance is that this orbital appears to form a much stronger overlap in the case of the hydride complex **26**, compared to the other two complexes, explaining the increase in the Berry pseudorotation observed earlier. A better π -backbond should result in more rigidly coordinated dmpe groups, and concomitant increased energy requirements for their exchange facilitated by BSR (Fig. 9 and 10).

The catalytic activity of complex **26** was investigated towards ketone hydrosilylation for a variety of substrates bearing different steric and electronic properties. What is noteworthy

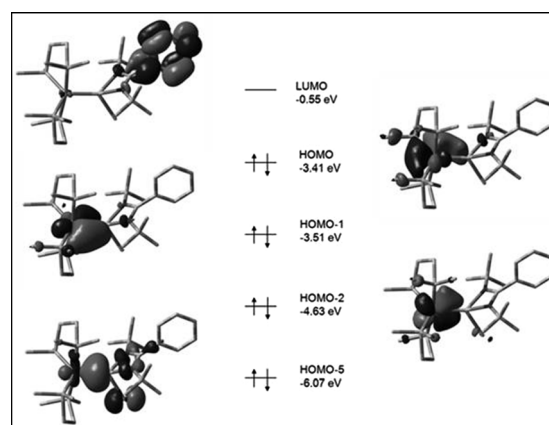


Fig. 9 Calculated boundary surfaces of some key frontier MOs and their respective energies in complex **25**. Complex **27** was found to exhibit analogous frontier MOs (adapted from ref. 16).

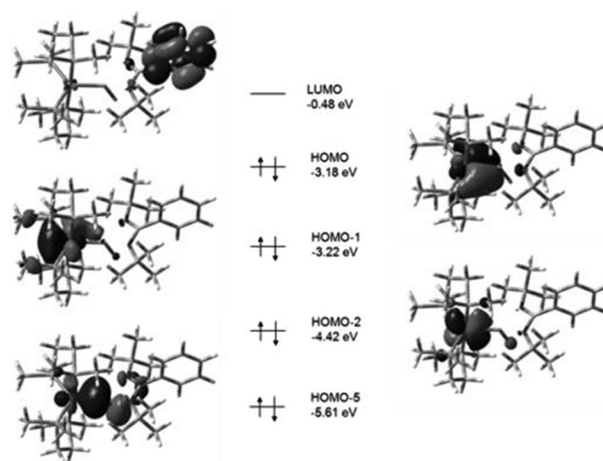
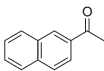
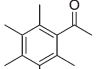
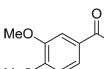
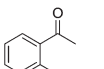
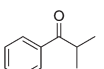
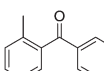
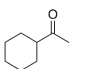


Fig. 10 Calculated boundary surfaces of some key frontier MOs and their respective energies in hydride complex **26**. The HOMO orbital clearly exhibits enhanced overlap compared to that observed in the related complexes **25** and **27** (adapted from ref. 16).

Table 4 Reaction conditions: pre-catalyst (5.0 mol%), substrate (0.16 mmol), (EtO)₃SiH (0.24 mmol), 70 °C, 24 h. Yield determined by GC-MS using *n*-dodecane as an internal standard

Entry	Substrate	Yield [%]
1		92
2		73
3		>99
4		>99
5		98
6		98
7		95

is that this is the first study showing the catalytic ability of a Si(II) hydride complex, and also the first such example for an Fe-based NHSi complex (Table 4).

Some mechanistic investigations to gain insight into the elementary steps in the catalytic process were also carried out. In an attempt to isolate a plausible intermediate, a stoichiometric reaction of **25** with a ketone, in the absence of the hydride delivery agent, (EtO)₃SiH, was carried out in the hope of isolating [(dmpe)₂HFe←{;Si←[:O=C(CH₃)(naphthyl)]L}] (L = PhC(N*t*Bu)₂) (**28**), which is a rational first intermediate in the catalytic process. Despite several efforts the product could not be isolated preparatively, owing to its instability. Instead, an NMR experiment was carried out to monitor changes in the ¹H and ³¹P{¹H} NMR spectra over time. Heating a sample of **25** with a stoichiometric amount of naphthylmethyl acetone in toluene-*d*₈, indeed revealed the selective formation of a new iron hydride species, featuring a broad multiplet signal at δ = -13.94 ppm in the ¹H NMR spectrum, typical of a terminal iron hydride. Moreover, in the reaction, the ³¹P{¹H} NMR spectra over time revealed the selective formation of two triplet signals at δ = 62.2 and 75.7 ppm (²J(P,P) = 27 Hz) along with consumption of **25**. These results provide some, perhaps anecdotal, evidence of H migration from the silicon to the iron centre, mediated by the ketone coordination to the silicon centre. These results point to the fact that the NHSi ligand is not merely a spectator ligand in the catalytic process, but

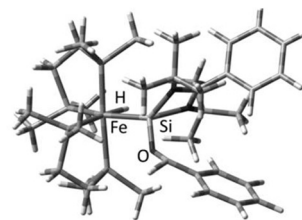


Fig. 11 Optimized structure of a simplified model (benzaldehyde as organic carbonyl) of **28** (**28b**). (B3LYP/6-31G(d) for C, H, N, Cl and Si; LANL2DZ for Fe).

mediates it. In addition to these experimental results, DFT investigations were also carried out to study the nature of the likely intermediate **28**. A slightly distorted octahedral structure could be located on the potential energy surface for a simplified model of **28** (**28b**), where benzaldehyde was employed (instead of the more demanding naphthylmethyl acetone) as carbonyl (Fig. 11).

A key feature of the structure of **28b** is a slightly elongated Fe-Si bond length (2.342 Å) compared to the calculated structure of the parent complex **26** (2.1976 Å), indicating reduced π-back-bonding from the iron centre to Si. In addition, the bond order is substantially reduced as reflected by the calculated Wiberg bond index from 1.1585 in complex **26** to 0.864 in **28b**. Noteworthy, the oxygen atom of the carbonyl is coordinated to the silicon centre and features a Si-O bond length of 1.6427 Å and a C-O bond length of 1.4495 Å. The latter parameter indicates elongation from a 'free' C=O bond to a C-O single bond character, which is hence the likely source of the C=O bond activation in the overall catalytic process. Moreover, the ketone oxygen atom forms a stabilising dative interaction with the even more electropositive silicon atom, following the H atom migration. What is noteworthy is that there is a substantial increase in the NBO charge on the Si atom in **28b** compared to **26** (Table 5), which indeed suggests that **28b** can be viewed as a "betaine-like" intermediate featuring a cationic Si atom, stabilised by the dative coordination of the ketone, along with an Fe(0) centre, bearing a negatively charged hydride ligand.

The yields of the isolated alcohols following work-up in all cases was excellent and even comparable to some existing benchmark systems for iron based ketone hydrosilylation.²¹

Taking these experimental and theoretical results into consideration, a possible catalytic mechanism was also presented by us in this report (Scheme 15).

Table 5 Comparison of Wiberg Bond Indices (WBI) values and the calculated Fe-Si distances of complexes **26** and **28b**. Level of theory: B3LYP/6-31G(d) for C, H, N, Cl and Si; LANL2DZ for Fe

Complex	NBO charge		WBI	<i>d</i> (Fe-Si) (Å)
	Fe	Si		
26	2.198	+1.237	1.1585	2.1976
28b	2.026	+1.935	0.864	2.342

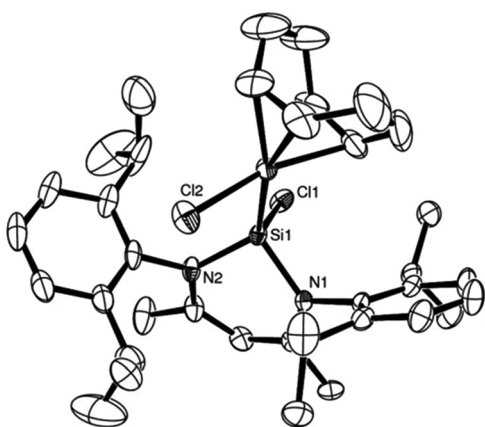
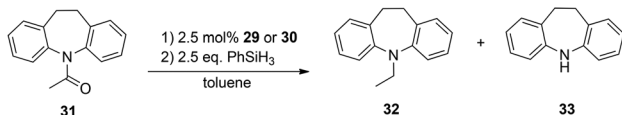


Fig. 12 ORTEP representation of complex **30:29** is isostructural; thermal ellipsoids at 50% probability, H atoms omitted for clarity (adapted from ref. 22).



Scheme 17 Reduction of a dibenzoazepine derivative **31** with complexes **29** or **30** as pre-catalysts.

The Rh–Si bond lengths in **29** are slightly shorter when compared to silyl rhodium complexes (2.32–2.38 Å), indicating some possible π -back-donation in **29**.²⁵ In close analogy, the Ir–Si distance of 2.3164(8) Å in **30** is within the typical range of other previously reported silyl iridium complexes²⁶ and nearly identical to another recently reported Ir based NHSi complex, from our group, bearing **3** as a ligand (2.3293(11) Å).²⁷

We next explored the catalytic activity of complexes **29** and **30** towards the catalytic reduction of amides. We selected this transformation given its current interest, and numerous reports from several groups, most notably by Milstein and Beller.²⁸

Based on these collective reports we decided to use the acetyl protected dibenzoazepine derivative **31** for our catalytic investigations with the novel NHSi Rh and Ir complexes **29** and **30** (Scheme 17). Two possible reductive products are a C–O cleavage product (**32**) and an N–C cleavage product (**33**).

By employing complex **29** as a pre-catalyst, selective C–O cleavage was observed and a conversion of the starting material to **32** in 61% yield. In contrast, for complex **30** under analogous catalytic conditions, both reductive products **32** and **33** were observed. Moreover, with the pre-catalyst **30** the total conversion of **31** is higher (87%) compared to **29** (Fig. 13 and 14).

For comparative purposes, we also tested the catalytic activity of the complexes ($[\text{Rh}(\text{Cl})\text{cod}]_2$, $[\text{Ir}(\text{Cl})\text{cod}]_2$) towards the reduction of **31** to gain insights into the effects the presence of the NHSi has on the catalyst activity and selectivity.²⁹ Indeed, the catalytic activity of $[\text{Rh}(\text{Cl})\text{cod}]_2$ is comparable to

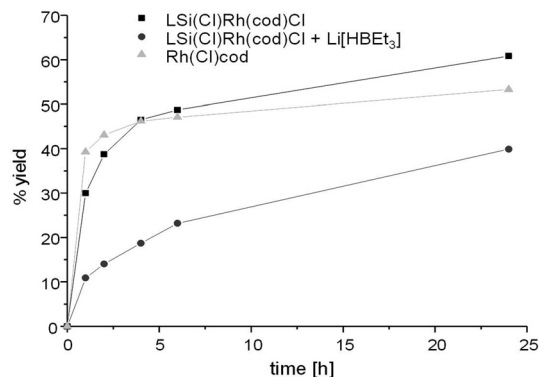


Fig. 13 Catalytic performance of complex **29** compared to $[\text{Rh}(\text{Cl})\text{cod}]_2$ as a function of time.

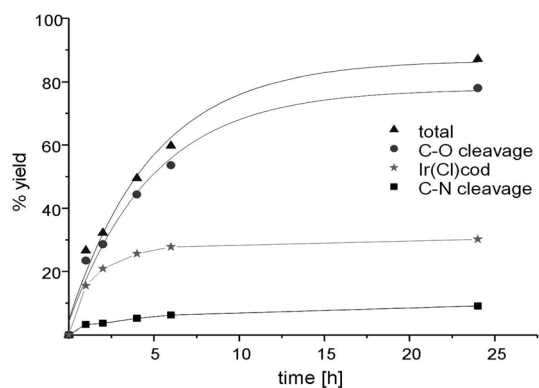


Fig. 14 Catalytic performance of complex **30** compared to $[\text{Ir}(\text{Cl})\text{cod}]_2$ as a function of time.

that of **29**. After 24 h a selective C–O cleavage of 53% was observed. Strikingly, however, the $[\text{Ir}(\text{Cl})\text{cod}]_2$ dimer shows considerably less activity after 24 h (30%) as compared to **30** (total: 87%, C–O cleavage: 78%, C–N cleavage: 9%) and the dimer exhibits a different chemoselectivity compared to **30**. The $[\text{Ir}(\text{Cl})\text{cod}]_2$ dimer as a pre-catalyst yields exclusively the C–O cleavage product, while **30** yields additionally the dibenzoazepine **33**. Therefore the coordination of the silylene ligand **3b** to the Ir centre increases the activity of the complex but at the same time affords both reductive products (Fig. 13 and 14).

Since hydride species have been implicated as important intermediates in the catalytic reduction of amides with other catalysts systems, we decided to probe the catalytic activity of complex **29** in the presence of a hydride source, $\text{Li}[\text{BHET}_3]$ (Fig. 13). The idea was to potentially generate the hydride analogue of **29** *in situ* by two hydride halide exchanges facilitated by $\text{Li}[\text{BHET}_3]$, which we thought could improve the catalyst performance.

Surprisingly, this action seems to retard the catalyst performance (Fig. 15), and this apparent deactivation pathway was also further explored by attempting to isolate the hydride analogue of **29**, compound **34**, on preparative scale.

This was attempted by reaction of **29** with two molar equivalents of $\text{Li}[\text{BHET}_3]$. Several attempts at isolating the potentially

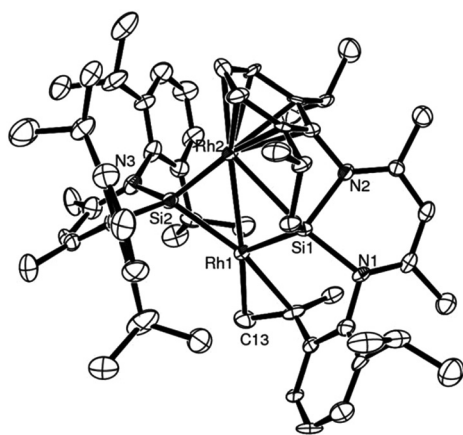
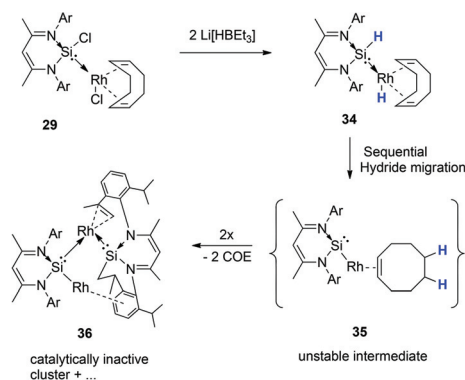


Fig. 15 ORTEP representation of complex **36**, one of the decomposition products resulting from the attempted transformation of **29** to **34**; H atoms omitted for clarity, thermal ellipsoids set at 50% probability (adapted from ref. 22).



Scheme 18 Attempted isolation of **34**, leading through COE elimination (observed spectroscopically) to a range of decomposition products, one of which (**36**) was identified by single crystal X-ray diffraction analysis.

reactive species **34** were however unsuccessful. Most likely, the inability to isolate this compound, is due to the migration of both H atoms (from Si and Rh, *via* 1,3 and 1,4H-shifts respectively) to the coordinated COE ligand, affording free COE, *via* an intermediate **35** (Scheme 18). This H migration was observed in repeated NMR scale experiments, where initial formation of Rh–H and Si–H signals is indeed observed, but then rapidly decays into the base line with concomitant formation of free COE and several other unidentifiable decomposed Rh complexes (Scheme 17, Fig. 15). One of these intractable decomposition products was characterized by single crystal X-ray diffraction studies (Fig. 15).

These results provide some explanation for the observed deactivation/retardation in the catalysis in the presence of Li[BHEt₃], since the *in situ* generated dihydride **34** is susceptible to COE loss and subsequent decomposition into intractable products which are most likely not catalytically active.

Finally, Inoue, Enthaler and co-workers have also recently reported the use of nickel complex [(cod)Ni←:6] (**37**) (cod =

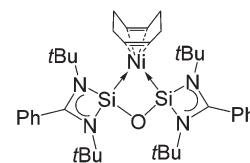


Fig. 16 Structure of bis-NHSi nickel complex **37**, capable of acting as a pre-catalyst in C–C cross-coupling reactions.

1,5-cyclooctadiene)^{6f} based on bis-NHSi ligand **6**, as a pre-catalyst in C–C bond formation reactions (Fig. 16).³⁰

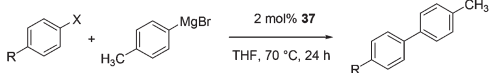
A series of C–C cross-coupling reactions were reported in this study with aryl halides and organometallic zinc and Grignard reagents. In most cases, good to outstanding catalytic rates were observed with **37** as a pre-catalyst.

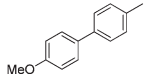
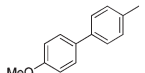
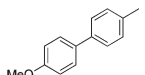
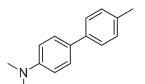
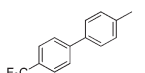
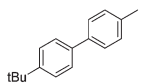
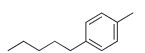
Some of these catalytic results are presented in Tables 6 and 7, respectively.

Table 6 Nickel-catalysed C–C bond formation of benzylzinc bromide with a variety of aryl halides^a

Entry	Substrate	Product	Yield [%]
1			98 (2)
2			29 (11)
3			8 (<1)
4			97 (<1)
5			74 (19)
6			49 (11)
7			85 (15)
8			>99 (<1)
9			>99 (<1)
10			<1

^a Reaction conditions: substrate (0.72 mmol), benzyl zinc bromide (1.08 mmol, 0.5 M in THF), pre-catalyst **37** (2.0 mol%), 70 °C, 24 h. The yield was determined by GC-MS and ¹H NMR. The yield of the homocoupling of the aryl halide is stated in parenthesis.

Table 7 Nickel-catalysed C–C bond formation of Grignard reagents with aryl halides^a


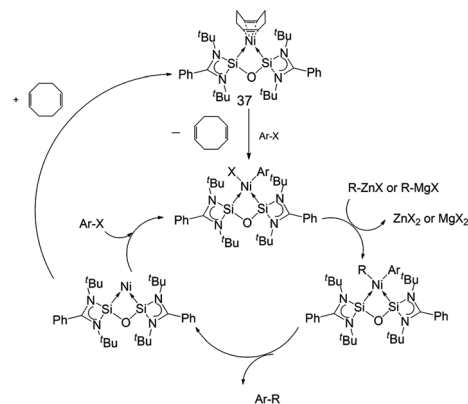
Entry	Substrate	Product	Yield [%]
1			63
2			74
3			79
4			72
5			93
6			61
7			<1

^a Reaction conditions: substrate (0.72 mmol), Grignard reagent (1.08 mmol, 1.0 M in THF), precatalyst 37 (2.0 mol%), 70 °C, 24 h. The yield was determined by GC-MS and ¹H NMR. (Yields of dehalogenated products and homocoupling products are omitted.)

The authors also present a mechanistic proposal for the coupling reactions based on previous mechanistic studies for other Ni-based catalysts. A reasonable mechanistic pathway potentially involves de-coordination of the cod from the precatalyst 37, as the first key elementary step, followed by oxidative addition of the arene halide over the Ni(0) centre. This affords a Ni(II) intermediate of the type 6:→Ni(R)X. Subsequent transmetalation with the Grignard or arylzinc reagent then generates the Ni(II) diaryl species 6:→NiRR' as the next step. Reductive elimination then affords the coupled product and regenerates the active Ni(0) species, closing the catalytic cycle (Scheme 19).

Conclusions

It is apparent from this short review that the use of N-heterocyclic silylene (NHSi) stabilised complexes in catalysis is still in its infancy but led already to a number of remarkable examples. The early stage of development of this research is

**Scheme 19** Mechanistic proposal for C–C cross-coupling mediated by 37, following a sequence of oxidative–addition/transmetalation/reductive elimination steps.

somewhat surprising, given that NHSi ligands are isoelectronic to N-heterocyclic carbene (NHC) ligands, where literally thousands of reports detailing their use as supporting ligands in a plethora of catalytic processes across the periodic table have been reported.

The few reports that do exist in this context, from the seminal work of Fürstner and Roesky, and later from our efforts, do however show that NHSi ligands are not merely passive spectators, or isoelectronic replacements for NHCs or phosphines, but in some cases play a pivotal role in the catalyst cycle, activity and even selectivity. They have the ability to fine-tune the electronic situation at the metal centre, through stronger σ -donation, compared for example to traditional phosphines, and thereby improve catalytic activity, as exemplified by our contribution on iridium-based NHSi complexes. Some NHSis can even mediate processes through cooperative effects, as seems to be the case with our NHSi hydridoiron complex.

A systematic study of NHSi complexes across the transition metals and their capacity to perform novel catalytic transformations or perhaps improve existing transformations is certainly a worthwhile aim. We are convinced that the coming years will witness more developments in this new and invigorating research area. Future endeavours might include the exploration of early transition metal (group III or IV) NHSi complexes, and their suitability in homogeneous catalysis; or even f-block NHSi complexes, which in themselves are a rarity in the literature.³¹

Acknowledgements

We are grateful to the Deutsche Forschungsgemeinschaft (DR 226-17/2) and the Cluster of Excellence UniCat (sponsored by the Deutsche Forschungsgemeinschaft and administered by the TU Berlin) for financial support of this research. We thank M. Stoelzel, Dr S. Enthaler, and Prof. Dr S. Inoue for fruitful discussions in the preparation of this review.

Notes and references

- 1 G. Schmid and E. Welz, *Angew. Chem.*, 1977, **89**, 823, (*Angew. Chem., Int. Ed. Engl.*, 1977, **16**, 785).
- 2 See as selected recent reviews, with references therein: (a) L. Zhang and Z. Hou, *Pure Appl. Chem.*, 2012, **84**, 1705; (b) S. Budagumpi, R. A. Haque and A. W. Salman, *Coord. Chem. Rev.*, 2012, **256**, 1787; (c) C. Valente, S. Calimsiz, K. H. Hoi, D. Mallik, M. Sayah and M. G. Organ, *Angew. Chem., Int. Ed.*, 2012, **51**, 3314; (d) A. Correa, S. P. Nolan and L. Cavallo, *Top. Curr. Chem.*, 2011, **302**, 131; (e) A. Poulain, M. Iglesias and M. Albrecht, *Curr. Org. Chem.*, 2011, **15**, 3325; (f) N. Marion and S. P. Nolan, *Chem. Soc. Rev.*, 2008, **37**, 1776; (g) T. Strassner, *Top. Organomet. Chem.*, 2007, **22**, 125; (h) W. J. Sommer and M. Weck, *Coord. Chem. Rev.*, 2007, **251**, 860; (i) H. D. Velazquez and F. Verpoort, *Chem. Soc. Rev.*, 2012, **41**, 7032.
- 3 B. Blom, M. Stoelzel and M. Driess, *Chem.-Eur. J.*, 2013, **19**, 40.
- 4 These are in fact the first examples of base-free silylene complexes. See: (a) S. D. Grumbine, T. D. Tilley and A. L. Rheingold, *J. Am. Chem. Soc.*, 1993, **115**, 358; (b) S. D. Grumbine, T. D. Tilley, F. P. Arnold and A. L. Rheingold, *J. Am. Chem. Soc.*, 1993, **115**, 7884; (c) S. D. Grumbine, T. D. Tilley, F. P. Arnold and A. L. Rheingold, *J. Am. Chem. Soc.*, 1994, **116**, 5495.
- 5 C. Zybilla and G. Muller, *Angew. Chem., Int. Ed. Engl.*, 1987, **26**, 669.
- 6 (a) M. Denk, R. Lennon, R. Hayashi, R. West, A. V. Belaykov, H. P. Verne, A. Haaland, M. Wagner and N. Metzler, *J. Am. Chem. Soc.*, 1994, **116**, 2691; (b) M. Driess, S. Yao, M. Brym, C. van Wüllen and D. Lentz, *J. Am. Chem. Soc.*, 2006, **128**, 9628; (c) C.-W. So, H. W. Roesky, J. Magull and R. B. Oswald, *Angew. Chem., Int. Ed.*, 2006, **118**, 4052, (*Angew. Chem., Int. Ed.*, 2006, **45**, 3948); (d) S. S. Sen, H. W. Roesky, D. Stern, J. Henn and D. Stalke, *J. Am. Chem. Soc.*, 2010, **132**, 1123; (e) W. Wang, S. Inoue, E. Irran and M. Driess, *Angew. Chem., Int. Ed.*, 2012, **124**, 3751, (*Angew. Chem., Int. Ed.*, 2012, **51**, 3691); (f) W. Wang, S. Inoue, S. Yao and M. Driess, *J. Am. Chem. Soc.*, 2010, **132**, 15890; (g) W. Wang, S. Inoue, S. Enthaler and M. Driess, *Angew. Chem., Int. Ed.*, 2012, **51**, 6167; (h) L. Kong, J. Zhang, H. Song and C. Cui, *Dalton Trans.*, 2009, 5444; (i) P. Zark, A. Schäfer, A. Mitra, D. Haase, W. Saak, R. West and T. Müller, *J. Organomet. Chem.*, 2010, **695**, 398; (j) For more details about reactivity and properties of NHSis see: M. Assay, C. Jones and M. Driess, *Chem. Rev.*, 2011, **111**, 354.
- 7 A. Fürstner, H. Krause and C. W. Lehmann, *Chem. Commun.*, 2001, 2372.
- 8 M. Zhang, X. Liu, C. Shi, C. Ren, Y. Ding and H. W. Roesky, *Z. Anorg. Allg. Chem.*, 2008, **634**, 1755.
- 9 A. Brück, D. Gallego, W. Wang, E. Irran, M. Driess and J. F. Hartwig, *Angew. Chem., Int. Ed.*, 2012, **51**, 11478.
- 10 D. Gallego, A. Brück, E. Irran, F. Meier, M. Kaupp, M. Driess and J. F. Hartwig, *J. Am. Chem. Soc.*, 2013, **135**, 15617.
- 11 Reviews for Sonogashira cross-coupling reaction: (a) R. R. Tykwinski, *Angew. Chem.*, 2003, **115**, 1604, (*Angew. Chem. Int. Ed.*, 2003, **42**, 1566); (b) E. Negishi and L. Anastasia, *Chem. Rev.*, 2003, **103**, 1979; (c) R. Chinchilla and C. Nájera, *Chem. Rev.*, 2007, **107**, 874; (d) R. Chinchilla and C. Nájera, *Chem. Soc. Rev.*, 2011, **40**, 5084. Examples using Ni-based catalysts: (e) L. Wang, P. Li and Y. Zhang, *Chem. Commun.*, 2004, 514; (f) I. P. Beletskaya, G. V. Latyshev, A. V. Tsvetkov and N. V. Lukashev, *Tetrahedron Lett.*, 2003, **44**, 5011.
- 12 See as representative and recent examples (and references therein): (a) R. H. Morris, *Chem. Soc. Rev.*, 2009, **38**, 2282; (b) *Iron Catalysis in Organic Chemistry*, ed. B. Plietker, Wiley-VCH, Weinheim, 2008; (c) S. Gaillard and J.-L. Renaud, *ChemSusChem*, 2008, **1**, 505; (d) A. Correa, O. G. Mancheño and C. Bolm, *Chem. Soc. Rev.*, 2008, **37**, 1108; (e) B. D. Sherry and A. Fürstner, *Acc. Chem. Res.*, 2008, **41**, 1500; (f) R. M. Bullock, *Angew. Chem.*, 2007, **119**, 7504, (*Angew. Chem. Int. Ed.*, 2007, **46**, 7360); (g) C. Bolm, J. Legros, J. Le Paih and L. Zani, *Chem. Rev.*, 2004, **104**, 6217; (h) E. B. Bauer, *Curr. Org. Chem.*, 2008, **12**, 1341; (i) W. M. Czaplik, M. Mayer, J. Cvengros and A. Jacobi von Wangelin, *ChemSusChem*, 2009, **2**, 396; (j) S. Enthaler, K. Junge and M. Beller, *Angew. Chem., Int. Ed.*, 2008, **120**, 3363, (*Angew. Chem. Int. Ed.*, 2008, **47**, 3317); (k) S. C. Bart, E. Lobkovsky and P. J. Chirik, *J. Am. Chem. Soc.*, 2004, **126**, 13794; (l) M. Haberberger, E. Irran and S. Enthaler, *Eur. J. Inorg. Chem.*, 2011, 2797; (m) S. Enthaler, M. Haberberger and E. Irran, *Chem.-Asian J.*, 2011, **6**, 1613.
- 13 Only three examples exist: (a) Ref. 1; (b) W. Yang, H. Fu, H. Wang, M. Chen, Y. Ding, H. W. Roesky and A. Jana, *Inorg. Chem.*, 2009, **48**, 5058; (c) T. A. Schmedake, M. Haaf, B. J. Paradise, A. J. Millevolte, D. R. Powell and R. West, *J. Organomet. Chem.*, 2001, **636**, 17.
- 14 This complex was first prepared in the laboratory of Prof. Dr A. C. Filippou (University of Bonn), by the first author of this publication in 2009. For the synthesis and full characterization see: B. Blom, *Reactivity of Ylenes at Late Transition Metal Centres*, Doctoral thesis, University of Bonn, Cuvillier Verlag, 2011.
- 15 [Fe(dmpe)₂(PMe₃)] reacts with germlylenes and stannylenes of the type RECl (E = Ge or Sn, R = 2,6-Mes₂-C₆H₃ or 2,6-Trip₂-C₆H₃; Mes = 2,4,6-Me₃-C₆H₂, Trip = 2,4,6-ⁱPr₃-C₆H₂) affording by PMe₃ elimination complexes of the type [(dmpe)₂Fe=ECI(R)], which can also be converted to triply bonded complexes: [(dmpe)₂Fe≡E-R]⁺A⁻.
- 16 B. Blom, S. Enthaler, S. Inoue, E. Irran and M. Driess, *J. Am. Chem. Soc.*, 2013, **135**, 6703.
- 17 H. Tobita, A. Matsuda, H. Hashimoto, K. Ueno and H. Ogino, *Angew. Chem., Int. Ed.*, 2004, **43**, 221.
- 18 R. G. Bryant, *J. Chem. Educ.*, 1983, **60**, 933.
- 19 For a leading reference on the Hammett constant see: C. Hansch, A. Leo and R. W. Taft, *Chem. Rev.*, 1991, **91**, 165.
- 20 H. A. Bent, *Chem. Rev.*, 1961, **61**, 275.

- 1 21 As a leading reference see: K. Junge, K. Schröder and M. Beller, *Chem. Commun.*, 2011, **47**, 4849.
- 22 M. Stoelzel, C. Praesang, B. Blom and M. Driess, *Aust. J. Chem.*, 2013, **66**, 1163.
- 5 23 M. Ahmed, C. Buch, L. Routaboul, R. Jackstell, H. Klein, A. Spannenberg and M. Beller, *Chem.–Eur. J.*, 2007, **13**, 1594.
- 24 E. Neumann and A. Pfaltz, *Organometallics*, 2005, **24**, 2008.
- 25 M. Aizenberg, J. Ott, C. J. Elsevier and D. Milstein, *J. Organomet. Chem.*, 1998, **551**, 81.
- 10 26 J. Y. Corey and J. Braddock-Wilking, *Chem. Rev.*, 1998, **99**, 175.
- 27 A.-K. Jungton, A. Meltzer, C. Präsaug, T. Braun, M. Driess and A. Penner, *Dalton Trans.*, 2010, **39**, 5436.
- 15 28 (a) G. W. Gribble, *Chem. Soc. Rev.*, 1998, **27**, 395; (b) J. Seyden-Penne, *Reductions by the Alumino- and Borohydrides in Organic Synthesis*, Wiley, New York, 2nd edn, 1997; (c) M. Igarashi and T. Fuchikami, *Tetrahedron Lett.*, 2001, **42**, 1945; (d) S. Das, D. Addis, S. Zhou, K. Junge and M. Beller, *J. Am. Chem. Soc.*, 2010, **132**, 1770; (e) R. Kuwano, M. Takahashi and Y. Ito, *Tetrahedron Lett.*, 1998, **39**, 1017; (f) R. Goikhman and D. Milstein, *Chem.–Eur. J.*, 2005, **11**, 2983; (g) N. Schneider, M. Finger, C. Haferkemper, S. Bellemin-Laponnaz, P. Hofmann and L. H. Gade, *Angew. Chem., Int. Ed.*, 2009, **48**, 1609; (h) E. Balaraman, B. Gnanaprakasam, L. J. W. Shimon and D. Milstein, *J. Am. Chem. Soc.*, 2010, **132**, 16756; (i) S. Krackl, C. I. Someya and S. Enthaler, *Chem.–Eur. J.*, 2012, **18**, 15267.
- 10 29 In fact this has been reported by Brookhart: C. Cheng and M. Brookhart, *J. Am. Chem. Soc.*, 2012, **134**, 11304.
- 30 C. I. Someya, M. Haberberger, W. Wang, S. Enthaler and S. Inoue, *Chem. Lett.*, 2013, **42**, 286.
- 15 31 See as a seminal example: W. J. Evans, J. M. Perotti, J. W. Ziller, D. F. Moser and R. West, *Organometallics*, 2003, **22**, 1160.
- 20
- 25
- 30
- 35
- 40
- 45
- 50
- 55